Energy Equip. Sys./ Vol. 12/No. 3/September 2024/ 249-262

ENERGY EQUIPSYS

Energy Equipment and Systems

www.energyequipsys.com

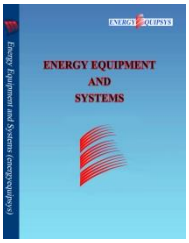

Actuator disk modeling for a wind farm in complex mountainous terrain: A case study

Manuscript Type

Research Paper

Authors

Mohammad Reza Ghasemi Bousejin[a,b*]
Kobra Gharali[c,d]
Bernhard Stoevesandt[e]
Joachim Peinke[b]
Seyed Saeid Mohtasebi[a]
Ali jafari[a]

[a] College of Agriculture and Natural Resources, University of Tehran, Iran

[b] ForWind-Centre for Wind Energy Research, Institute of Physics, University of Oldenburg,Oldenburg, Germany

[c] Mechanical Engineering Department, University of Tehran, Iran

[d] Waterloo Institute for Sustainable Energy (WISE), University of Waterloo, Waterloo, Canada

[e] Fraunhofer Institute for Wind Energy Systems, Küpkersweg , Oldenburg, Germany

ABSTRACT

For optimizing the operational efficiency of a wind farm in complex terrain, the wake study of wind turbines and the detailed analysis of the wind data are essential. In this research, The Manjil wind farm located in the Alborz Mountains with special topography and distinct wind regimes has been studied. OpenFOAM has been applied for computational fluid dynamics simulations of two wind speeds at different reference heights as case studies. Then, a comparison between the simulation results and the available supervisory control and data acquisition dataset was made. The result assumed that the velocity of the wake is recovered up to 85% after ten times the diameter of the turbine. In this distance, there is a 14.5% and 15.5% speed reduction on average for two simulations, with velocity on the hub height of 9 and 17 m/s respectively. The analysis of raw wind data shows that a high potential of wind energy is available in summer and there is almost no wind in wintertime, which causes some challenges for developing the wind farms under these conditions.

Article history:

Received : 10 June 2023
Revised : 26 May 2024
Accepted : 1 June 2024

Keywords: Actuator Disk Model, Mountainous Terrain, Far Wake, Wind Turbine, Wind Farm.

1. Introduction

With the increasing importance of wind energy for the world's future (IPCC, 2014) [1], distinct geographical regions such as mountainous areas with high potential for wind energy have been brought to attention. The study of wind farms located on complex terrains is essential due to its complicated parameters. The wake effect of turbines in wind farms is a crucial parameter for optimization, especially in complex terrain. Numerical simulation of wind farms is a useful

Corresponding author: Mohammad Reza Ghasemi Bousejin
Mechanical Engineering Department, University of Tehran, Tehran, Iran
E-mail: mrghasemib@gmail.com

method and could be compared with experimental data.

The flow field studies of a wind farm are challenging since many parameters such as surface roughness, area topography, and wind turbulence levels influence the results. The velocity deficit behind a turbine rotor reduces the available wind energy for downstream turbines resulting in power reduction. Upstream wind turbines increase turbulence intensity causing negative effects on the fatigue life of the downstream turbines (Matteulla et al, [2]).

Wind farms have been studied analytically, numerically and experimentally including either field measurements or wind tunnel measurements. Wind farm layout optimizations (WFLO) on flat terrains have been done by some approaches; however, optimizing wind farm layouts on complex terrains is challenging. Kuo et al, [3] proposes an algorithm that couples computational fluid dynamics (CFD) with mixed-integer programming (MIP) to optimize layouts on complex terrains. CFD simulations are used to iteratively improve the accuracy of wake deficit predictions while MIP is used for the optimization process. Results show that the proposed algorithm is capable of producing excellent layouts in complex terrains. Makridis and Chick, [4] investigated wind turbine wakes and the neutral atmospheric wind flow over complex terrain using the Computational Fluid Dynamics software Fluent.

Linear models were not suggested for complex terrains (Matteulla et al, [2]) due to complicated wind regimes particularly in hill wakes and highly turbulent areas; instead, Computational Fluid Dynamics (CFD) methods in particular combined with experimental methods have been applied in the wind energy industry. The Atmospheric Boundary Layer (ABL) for wind study can be simulated successfully in this method.

The prediction of local ABL characteristics and its interaction with wind turbines are important for wind farm optimizations. Mattuella et al [2] combined an experimental method with a proper simulation for an ABL study over a complex area. Their research describes an experimental simulation of the ABL in a wind tunnel over a complex terrain. They presented the contribution that wind tunnels have made to physical modelling. Their results demonstrated that the mean velocity and the turbulence intensity vary significantly over the complex area. Kozmar et al [5] simulated an ABL for a flat terrain as a reference case and then carried out some wind tunnel experiments to analyze the wind turbine wakes located downwind of a mountain. They studied wake characteristics of a single wind turbine model in the wake of various terrain models including flat terrain, small mountain, large mountain, mountain with a bay. The mountain-induced flow disturbance is enhanced with increasing the size and complexity of the mountains. Turbulence intensity in the wake of the mountain and wind turbine was considerably larger than in the ABL and velocity power was highly influenced by the terrain complexity.

For the wind farm assessment, the rotor of a wind turbine can be replaced by an actuator disk. The Reynolds-averaged Navier–Stokes (RANS) method can be utilized for the simulation. The concept of the Actuator Disk model (ADM) is based on an ideal disk with an appropriate pressure drop across it and wind energy extraction according to the induction. ADM is practical and cost-effective (Castellani & Vignaroli [6]) and has been used extensively for CFD studies of wind farms. Choi et al, [7] had done (CFD) study of a wind farm with two sets of wind turbines. CFD analysis was calculated by using the CFD solver ANSYS CFX. Blade design and modelling were based on blade element momentum theory. The results showed that there was a power output difference due to the wake effect between two wind turbines. A complete wind farm mesh is generated including the rotor, nacelle and tower.

Porte-Agel et al [8], in a study, developed a Large-Eddy simulation (LES) method for wind energy applications. They used two models for the load calculation over the rotor: ADM and actuator-line model (ALM). Their results showed good agreement with the wind tunnel measurements in the far wake regions. Their results of ADM, without rotation, were able to capture the velocity distribution in the far wake but the velocity in the center of the wake in the near wake region was overpredicted slightly. LES is a promising approach for simulating the site-specific characteristics of turbine wakes in complex terrains; however, even with the recent generation of supercomputers, LES is extremely costly and sometimes impossible for a wind farm simulation (Yang et al, [9]).

Castellani and Vignaroli [6] used ADM numerically in order to simulate the wakes of an offshore wind farm in Windsim working with an orthogonal Cartesian grid. Their results demonstrated that ADM can provide useful information for wind farm studies in coastal areas. Then, Castellani et al [10] studied a wind farm located in flat terrain and another one located in complex terrain with two different numerical methods, including CFD and mass consistent modelling. Their numerical results were compared and validated with measured data from a met-masts anemometer and from Supervisory control and data acquisition (SCADA) control systems. The studies showed the usefulness of the method for wake simulations.

To determine the potential of the wind resource of a site, a set of measurements are to be taken as well as nearby long-term measurement stations (Frank et al, [11]).

In this paper, a wind farm in complex terrain has been simulated numerically using ADM with OpenFOAM code. This open-source software and simulation for complex terrain has been adapted with a developed code in this research. The mesh grid had generated for real topography of a wind farm which was not studied previously. Then SCADA data of wind farm has been analyzed and compared with the simulation results for validation.

The current wind farm study comes from a collaboration between the University of Tehran, Fraunhofer Institute, and ForWind center at the University of Oldenburg.

Nomenclature

X	direction in span-wise
Y	direction in stream-wise
Z	direction in vertical
L_X	domain size in X direction, m
L_Y	domain size in Y direction, m
L_Z	domain size in Z direction, m
X/D	dimensionless distance in X direction
Y/D	dimensionless distance in Y direction
Z/D	dimensionless distance in Z direction
T_1	turbine number 1
S_1	met mast number 1
D	turbine rotor diameter, m
v	wind velocity, m/s
z	height that wind velocity calculated, m
v_{ref}	wind velocity at the reference height, m/s
z_{ref}	reference height, m
z_0	terrain surface roughness, m

2. Manjil wind farm

Manjil wind farm was selected as a proper option for the current study. Manjil wind farm installation was started in 1994 in the Alborz mountains in the northern part of Iran (Fig.1a). At the wind farm, there are special wind conditions with strongly intermittent wind from one main direction.

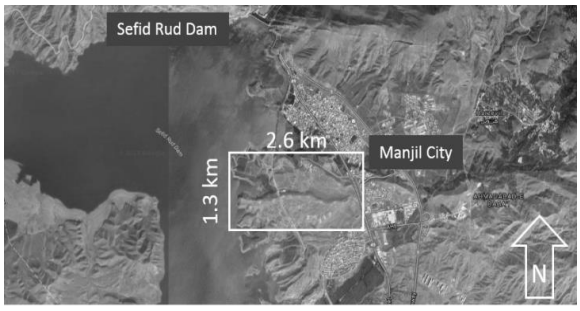

a) Manjil wind farm location (google maps 2016)

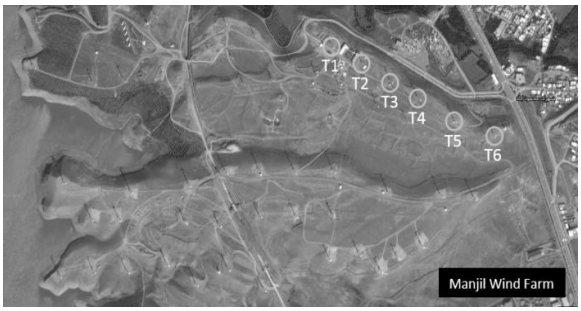

b) Close view of simulated wind turbines

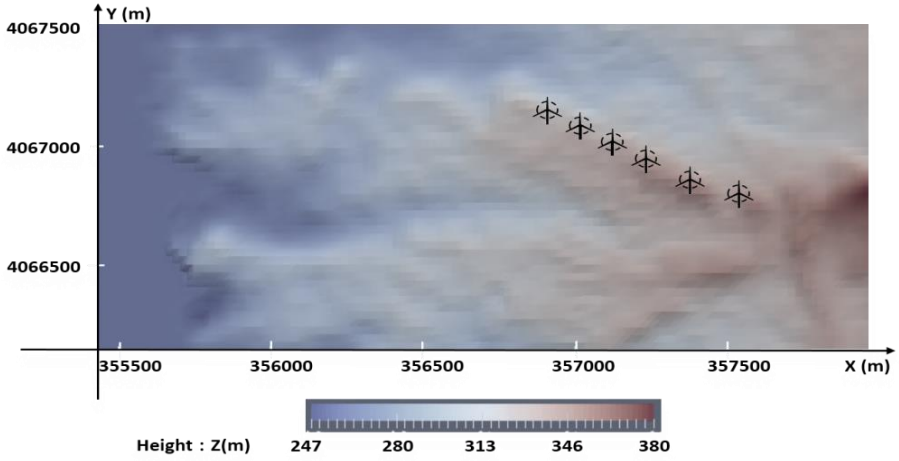

c) Wind farm topography with marked locations of simulated wind turbines (USGS 2016)

Fig. 1. Layout of Manjil wind farm

The wind farm with a size of 2600 x 1300 m^2 is located in the valley of high mountains in Manjil, Guilan province in Iran. The wind farm consists of 52 wind turbines of different sizes. This research focuses on the simulation of ABL flow and its interactions with six wind turbines located in the first row of the wind farm as shown in Fig. 1b. Since only for one turbine of the first row , called T5 in this study, real data is available, the focus of the simulation is on the first row of the turbines including T5. The wake of the first row can affect the next rows because of the wind direction.

In Fig. 1c and Table 1, the X-Y coordination of 6 turbines is provided. In Table 1, turbine hub heights are measured from the sea level considering the wind farm topography.

There are five Nordtank NTK 550 turbines, including T2 to T6, with a rotor diameter of 41 m and a hub height of 42 m in the first row. The other turbine (T1) in the first row is smaller than the rest (NTK 500). For the simulation, all six turbines are assumed to be the same with 550 output power. However, T1 can not have too much impact on T5 because of the wind direction as shown in wind rose (Fig. 2).

3. Wind data and simulation case study

Manjil wind farm in the Alborz mountains is also close to the Caspian Sea. The geographical location of this wind farm causes a very complicated wind regime.

Available wind data for this wind farm are gathered from two sources (Astolfi et al, [12]):

1) Data from the Iran Meteorological Organization with the precision of 1 m/s for the wind speed and 10 degrees for the wind direction. Data were recorded by a met mast tower of a weather forecasting station in Manjil city (Table 1). Met mast (S1) was located at a height of 10 m above the earth in a measurement tower.

2) SCADA data gathered in the wind farm. Data were recorded every 10 minutes with a precision of 0.1 m/s for the wind speed on wind turbines (the rotor effects were ignored).

The wind rose for S1 data shows that the dominant wind blows from the north (Fig. 2). Around 54% of useful incoming wind (with a speed of more than 4 m/s) blows from the north. Also, around 13% of useful incoming wind tilts 30-degrees from north to northeast direction). As a result, the north-south direction has been chosen as the reference direction in the simulation. With these simulations, it was expected to cover the most relevant situations in the wind farm. This is due to the very unique wind conditions in the wind farm. Since the location of the measurement mast (S1) is lower than the T5 hub height, the wind speed at the T5 hub height should be estimated from S1 Data (Seim et al, [13])

Table 1. The information of wind turbines and met mast positions in the X-Y Coordinate system

Turbine number	height (m) *	X (m)	Y (m)
T1	367.60	356910	4067104
T2	374.00	357021	4067043
T3	377.61	357128	4066978
T4	389.66	357239	4066911
T5	394.85	357385	4066826
T6	384.71	357543	4066774
S1	348.30	357106	4064635

* Hub height is added to the earth height where the turbine is installed. met mast height is 10 m above the earth height where the met mast tower is installed.

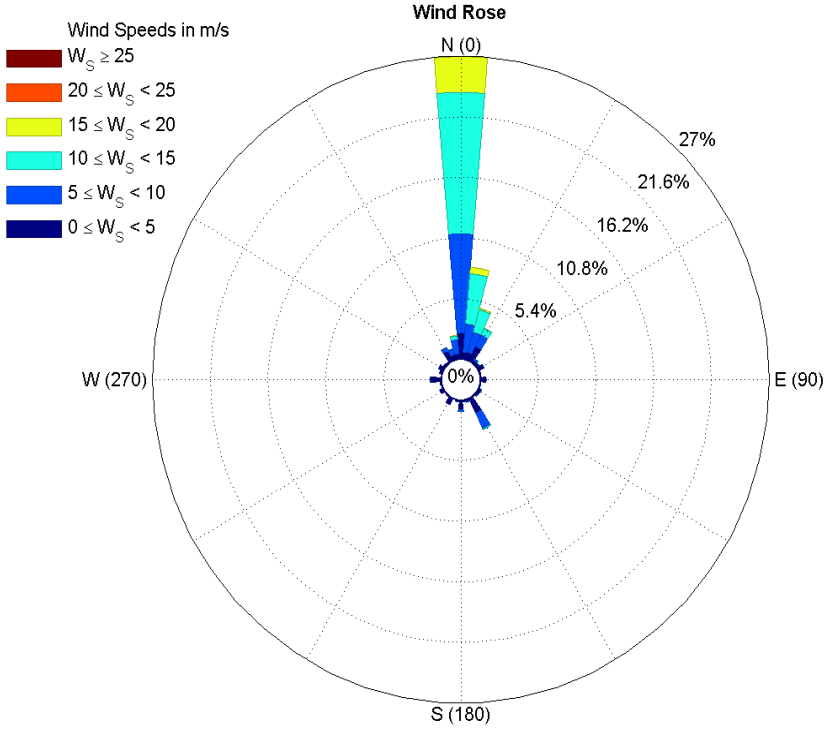

Fig. 2. Wind rose

Based on the input velocity (obtained from wind rose), two cases have been selected for the simulations (Table 2). The two cases are representative of average and high wind speeds. Considering to inlet velocity in selected heights in Table 2, the inlet profile was obtained and implemented in simulation as the inlet condition. For that, the logarithmic formula given by (Burton et al, [14])

$$v = v_{ref} \frac{ln\left(\frac{z}{z_0}\right)}{ln\left(\frac{z_{ref}}{z_0}\right)} \quad (1)$$

is used, where v is the velocity (m/s) at height z *(m)* and v_{ref} is the velocity at the reference height z_{ref}. Since the land is covered by small bushes, few trees and obstacles, the surface roughness length, Z_0 is assumed 0.05 m. The inlet profiles implemented for the North part of the domain as incoming wind (Fig. 3).

The wind speed on turbine T5 (with a hub height of 394.85 m) is available from SCADA data which is considered as the reference point.

For case study 1, with an inlet velocity of 8 m/s, the velocity on the hub of T5 is calculated from simulation around 9 m/s. This is approximately equal to the average wind speed for one year from SCADA data for T5.

Table 2. Case studies

	Inlet conditions for the simulation		Reference point at the T5 hub	
	Height (m)*	Velocity (m/s)	Height (m)*	Calculated velocity (m/s)
Case study 1	340	8	394.85	9
Case study 2	310	12	394.85	17.1

* The lowest earth level in the simulated area for the wind farm is around 300 m

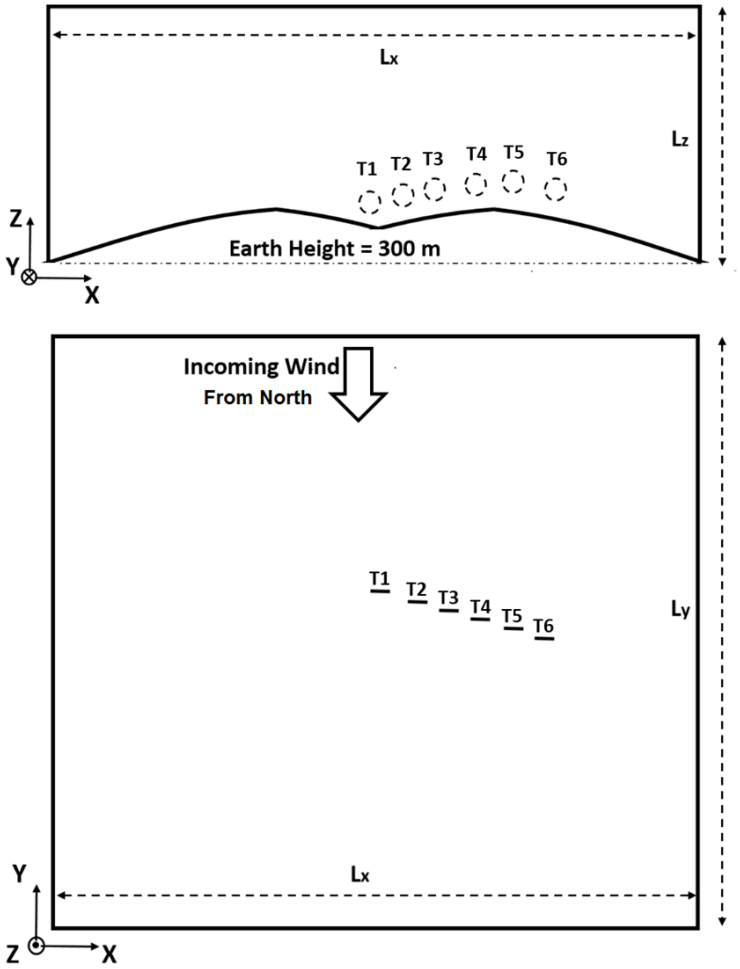

Fig. 3. Schematic representative of the domain

Therefore, case study 1 is based on average wind speed for one year. For case study 2, the input velocity for the simulation is 12 m/s. In this case, the calculated velocity of T5 is 17.1. This speed is in the range of high speed seen by T5 in the summer time. Also, it is above the rated speed of the wind turbine. (It described in SCADA data analysis).

4. Numerical simulation

The mesh generation and simulation have been done by OpenFOAM software. The code was extended for the wind farm simulation in Fraunhover institute (IWES) in Oldenburg, Germany.

4.1. Mesh generation

The map of the wind farm obtained from the U.S Geological Survey (USGS) as a tiff file in June 2016. The tiff file was converted to a stl file. The stl file covers the area of 2600 m (X direction) and 1300 m (Y direction) which is equal to the wind farm area shown in Fig. 1c. To achieve converged results, the mesh domain should be increased

slightly. The final domain size is L_x=4600 m, L_y=5300 m and L_z=2000 m in the X (spanwise), Y (streamwise) and Z (vertical) directions, respectively (Fig. 4a). L_z is chosen 2 km to allow full ABL development. In the vertical, z direction, the boundary layer mesh is generated with an aspect ratio of 1.15. The ground mesh dimension in the X-Y plane is 15x15 m^2 in the area of the wind farm. Applied mesh dimension (15 m resolutions) presents an acceptable mesh independency comparing with two different sizes of 12 m and 20 m which shows 1% and 6% deviation for wind speed in turbine hub height, respectively. Around each wind turbine, three refined boxes are generated with a mesh refinement in all directions. The sizes of the boxes are 200x200x150 m^3 (the size of the first box), 120x120x120 m^3 (the size of the second box) and 80x80x80 m^3 (the size of the third box), Fig. 4b.

Using the software functions, the described background mesh for the whole domain was generated by terrainMesherDict; then mesh was refined for the critical zones and actuator disks were added into the domain (Schmidt and Chang, [15,16]). The atmospheric boundary layer was created by ablBoundaryFoam code. The final mesh size was 1997100 Cells.

Wall condition option for the ground side of the domain and patch condition (generic type in OpenFOAM) for the Inlet, the outlet and other sides of the boundary had implemented.

4.2. Solver

An extended code in the OpenFOAM software called ablSimpleFoam solved the whole domain with 12 processors in the central cluster of the University of Oldenburg. The k-epsilon turbulence model was selected for all the simulations. Equation had been solved in steady condition with Reynolds number above 10 millions and a time step of 1 second.

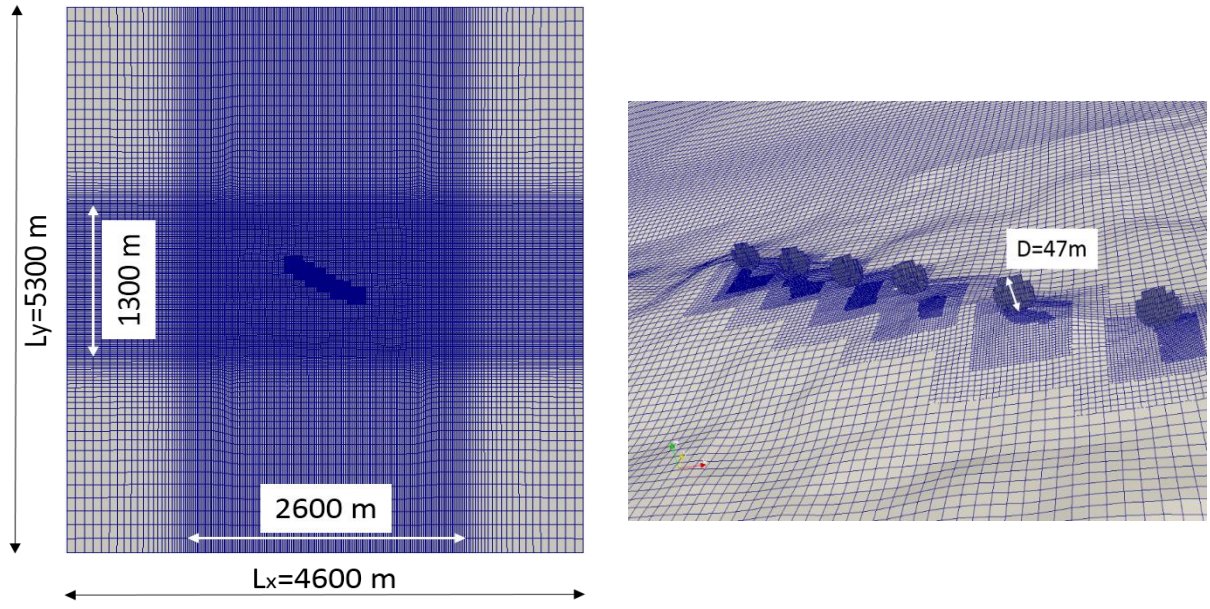

Fig. 4. Structural mesh of wind farm (a) the whole domain (b) close view of final ground meh and turbines mesh

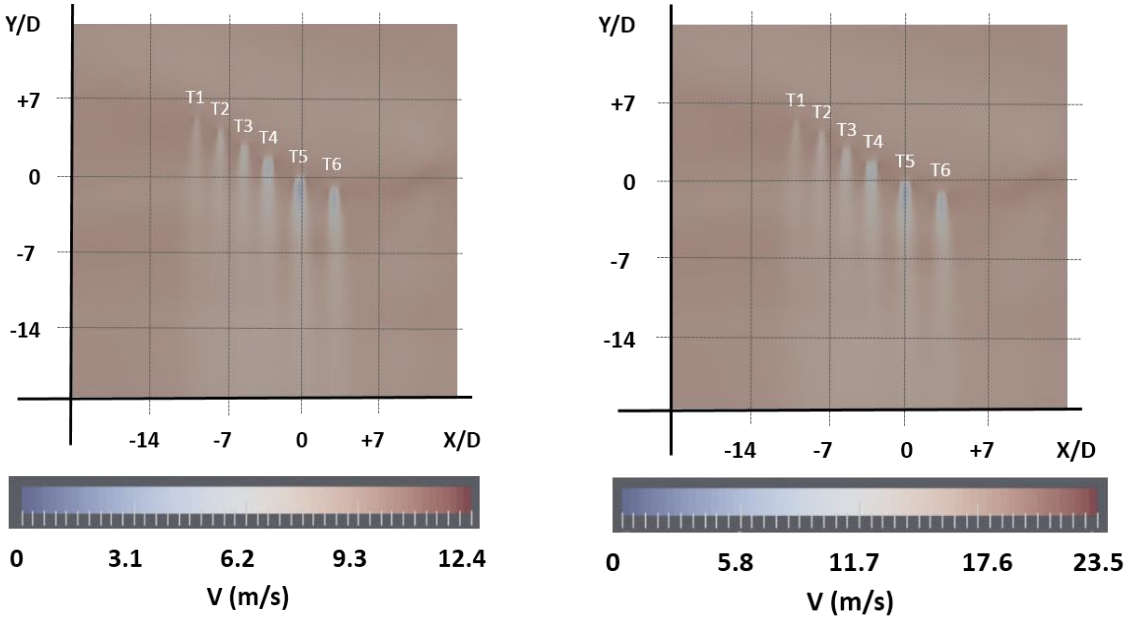

a b

Fig. 5. Velocity contours at the height of 400 m in wind farm for (a) case study 1 (b) case study 2

Since the predominant wind was from the north (see wind rose in Fig. 2), only the north wind has been selected for the simulations.

5. Results and discussions

Simulation results will be shown and discussed for wind turbines and then in the next section, SCADA data for available T5 will be analyzed and its results will be compared with simulation results for validation.

Simulation results for wind turbines

The velocity contours around six turbines are shown for case study 1 and case study 2 in Figs 5a and 5b, respectively. The contours are obtained from a section cut, in height of 400 m from the sea level. Ria et al [17] had chosen the average elevation to present contours. The hub of the highest turbine, T5, is located at 394.85 m from the sea level. Thus, the speed reduction behind T5 is more visible as it is occurring closer to the hub height. It is going less as much as far away from hub height. Then, it is less visible in T1 due to its more distance of hub height from the section cut. for the details of the other turbine heights see Table 1). The (Y/D) axis in Fig. 5 demonstrates the distance from T5 over the turbine diameter, D. It reaches from +14D before T5 to -21D behind T5. The (X/D) is the same as (Y/D). Characteristics of the wake show an extension of the wake even more than 10D downstream.

In Fig. 5a, the maximum velocity reaches 12.4 m/s. in Fig. 5b, the highest velocity is 23.5 m/s. For both cases, as expected, the six wind turbines were installed in the region with high wind regime located on the top of the hill agreeing well with Fig. 1c, where the turbines are located in proper heights.

In Fig. 5, the most notable issue is that the wakes of the simulated turbines in the first row do not interact with each other much up to 10D. Thus T5 (As turbine with complete field data for validation) is not influenced by any of the other turbines in the relevant wind directions. This offers the possibility of installing second-row turbines between upstream wakes.

Figs 6 and 7 show the velocity profiles in different locations (from 1D before T5, (Y/D = +1) to 10D after that (Y/D = -10)) for case studies 1 and 2, respectively. In Fig 5 the magnitude of wake deficit is big by 5D and The wake deficit is clear by the far wake (Y/D more than 5). It is not important after 10D with the wake velocity close to the upstream velocity proven in Figs 6 and 7. The magnitude of the wake velocity reaches close to the incoming wind speed at the distance of 10D which agrees well with the simulation results of Porte agle et al [8]. They used ADM without rotation similar to the current method. Moreover, From their

results, the velocity deficit was visible even for Y/D=20 similar to the current study.

In Figs 6, wind speed at hub height is around 9 m/s in Y/D = +1 and it had reduced significantly in Y/D = -1, -2, -3 and is around 4 m/s due to the turbine effect. It had recovered slightly by Y/D = -5 and is around 6.6 m/s. finally at Y/D = -10 it had recovered significantly and is around 7.7 m/s and is close to inlet velocity, 9 m/s. speed reduction close to hub height is more and it had softened by going far from hub height.

In Figs 7, wind speed at hub height is around 17.1 m/s in Y/D = +1 and it had reduced significantly in Y/D = -1, -2, -3 and is around 8 to 9 m/s due to the turbine effect. The trend is similar to Figs 6 and it had recovered slightly by Y/D = -5 and is around 12.7 m/s. finally at Y/D = -10 it had recovered significantly and is around 14.4 m/s and is close to inlet velocity, 17.1 m/s.

In Figs 6 and 7, first profiles (wind profiles in a distance of 1D before T5) are assumed as the incoming wind profiles. A comparison of this velocity with the wake deficit is done for T5 and presented in percentage in Table 3.

Table 3. Wind speed reduction in the centerline of T5

Distance From T5	Wind Speed Reduction (%)	
	case study 1	case study 2
D	58%	56%
2D	54%	52%
3D	43%	42%
5D	26%	26%
10D	15%	16%

For 1D, there are 58% and 56% speed reductions for case study 1 and case study 2 respectively. The results for both case studies are slightly similar. however, the result shows that the wake speed is a bit more affected at the close wake for case study 1. On the contrary, in the far wake, the velocity of the wake of case study 1 is recovered a bit faster than that of case study 2. In Table 3, 15% and 16% speed reductions behind the hub center of T5 are shown for 10D. For the whole swept area of each rotor, there is a 14.5% and 15.5% speed reduction on average for case study 1 and case study 2 respectively. Installing second-row turbines in 10D exactly behind T5 could reduce the obtained power by 62.5% and 60% for the two cases respectively.

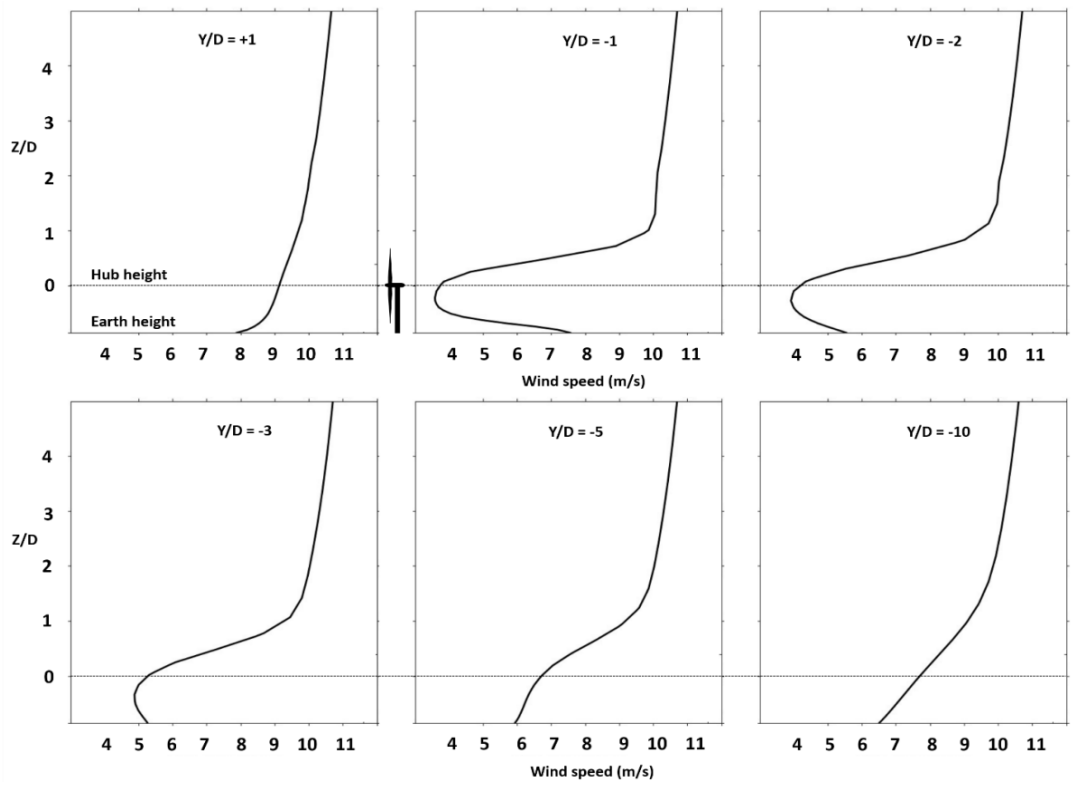

Fig. 6. For case study 1, wind speed versus the height at different distances from T5

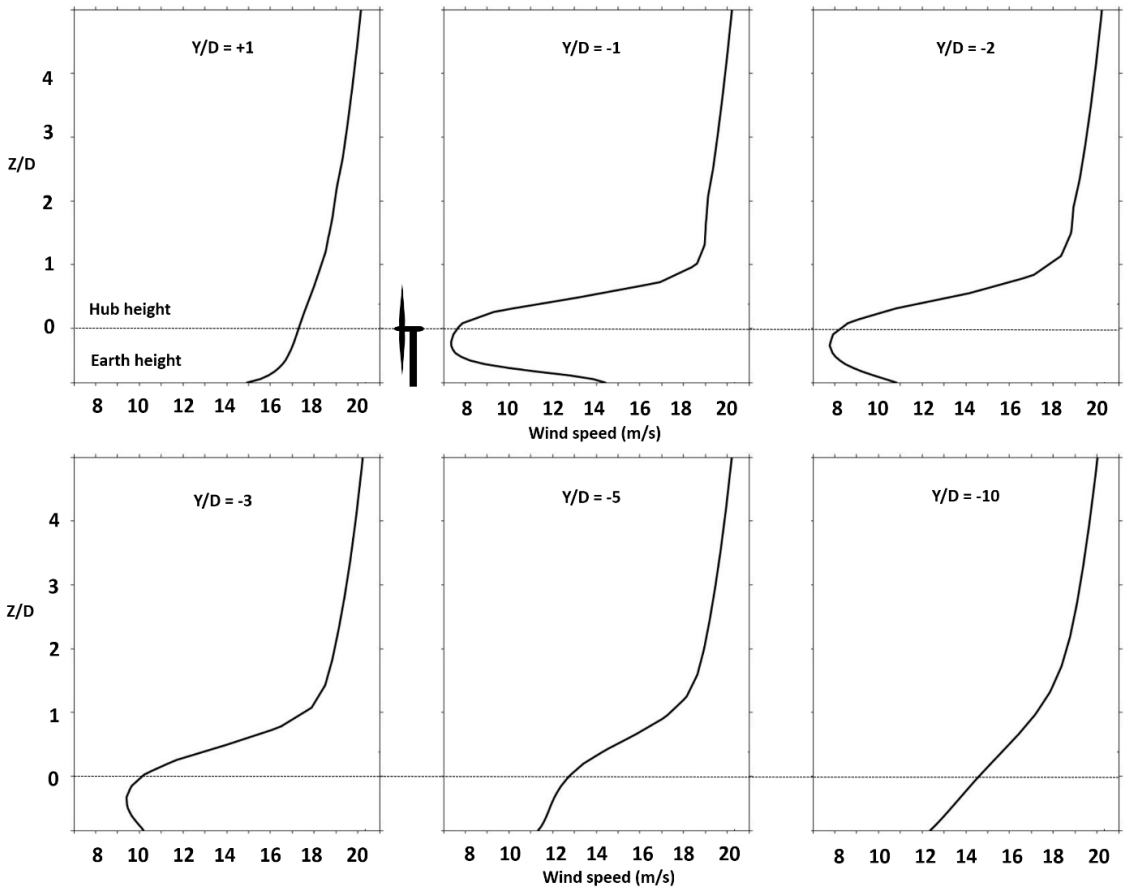

Fig. 7. For case study 2, Wind speed versus the height at different distances from T5

6. SCADA data analyzation for T5

SCADA raw data were available for the hub height of T5 for 2013. The data were recorded every 10 minutes for all months. After data filtering, the remained data were analyzed. The results are investigated for each month separately.

Table 4 presents the average wind speeds monthly. The overall wind speed average over the year is almost 9 m/s. The average wind speed is more than 10 m/s in June, July, August, and September. In November, December, and January, the average wind speed is around 4 m/s.

Due to the strong seasonal differences, further analysis for harvested power was done for 4 selected months. July has been chosen as a month with high wind speed and January for low wind speed (Figs. 8 and 9). Also, the average wind speeds in May and October are close to the average wind speed for all months, and thus shown in Figs. 8 and 9, and used for case study 1. All selected months include 31 days.

The reported harvested energy for T5 is available in Table 4. The average wind speed is a key point in gained wind energy, but wind speed fluctuations are also important. As a result, the maximum average wind speed, 14.7 m/s, occurred in July, but maximum wind energy was gained in August with a wind speed of 13.8 m/s on average.

Table 4. Monthly SCADA data for T5

month	Average wind speed (m/s)	Wind energy (Mwh)
January	4.4	77.5
February	5.7	102.9
March	7.3	133.2
April	9.7	175
May	8.9	156.5
June	12.9	221.1
July	14.7	246.5
August	13.8	255.5
September	11.2	193
October	8.7	164.5
November	3.8	66.1
December	4	68.6

In Fig. 8, the wind speed histograms show a significant deviation from typical Weibull statistics. This is most likely caused by the geographic conditions in theAlborz mountains as the Manjil wind farm is located in a valley spanned in the South-North direction. Wind blows from the Caspian Sea in the North toward the valley (according to Fig 2). Further, there is a critical difference in the wind regime for winter months versus summer months. In January, for significant periods, the wind blows below the cut-in speed (4 m/s) causing low average wind power generation. Power production in July comes from just a few separate windy days(Fig. 9). Since the air density is higher in cold weather, the maximum power generation peak in January is higher than that of in July. These high power generations occur for a short period in January with high fluctuations which are not well suited for grid connection. The wind speed fluctuations make the power prediction challenging. On the contrary, In July, the wind speed is almost constant close to the rated power (18 m/s) leading to a nearly constant power production of 450 KW with a few short fluctuations. In May and October, useful wind speeds are more than in January, However, fluctuation is high comparing to July. Power generated for May and October (Fig.9) shows the better result, with energy generated more than two times in January but around 63.4% and 66.7% of July, respectively (Table.4). Because of this special wind regime, there is no reason for operating the wind farm in the winter months such as January with the significant low wind speed.

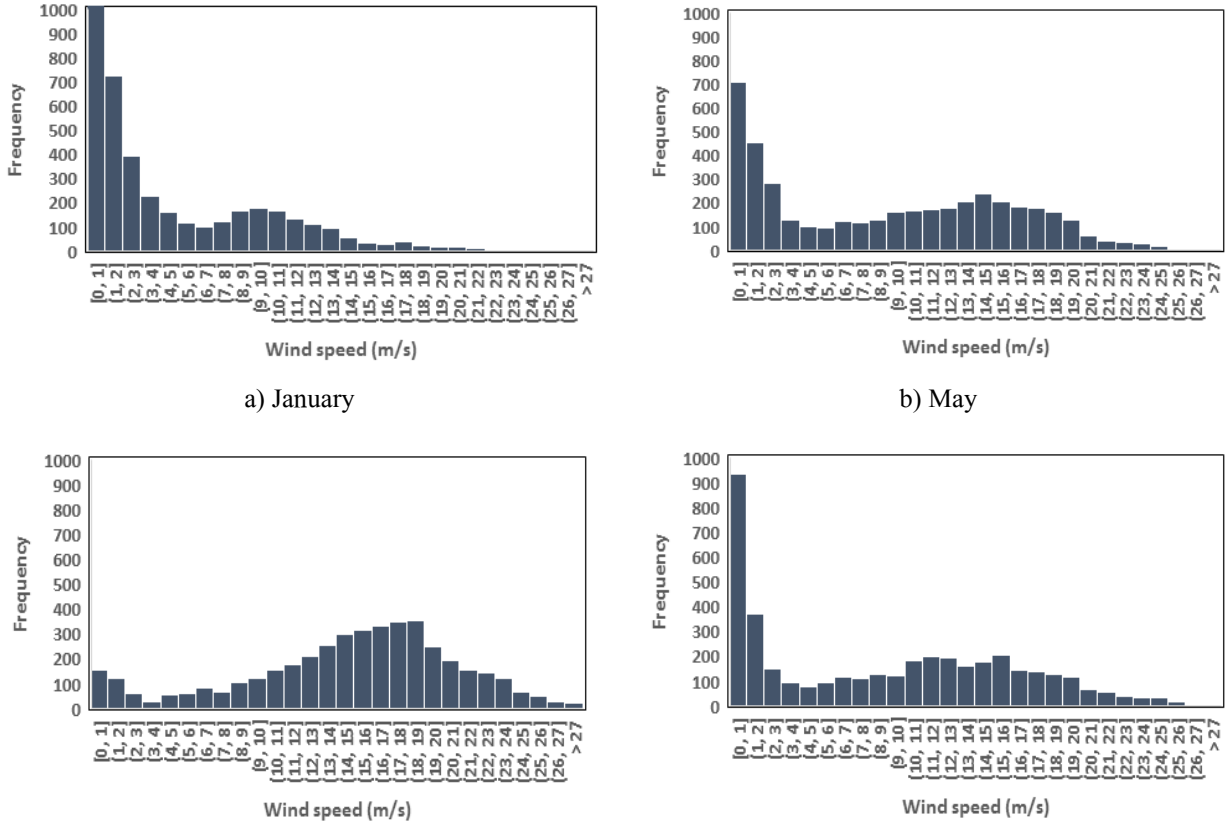

a) January b) May

c) July d) October

Fig. 8. Wind speed histogram in T5 in sample months of January, May, July and October of 2013 according to SCADA data.

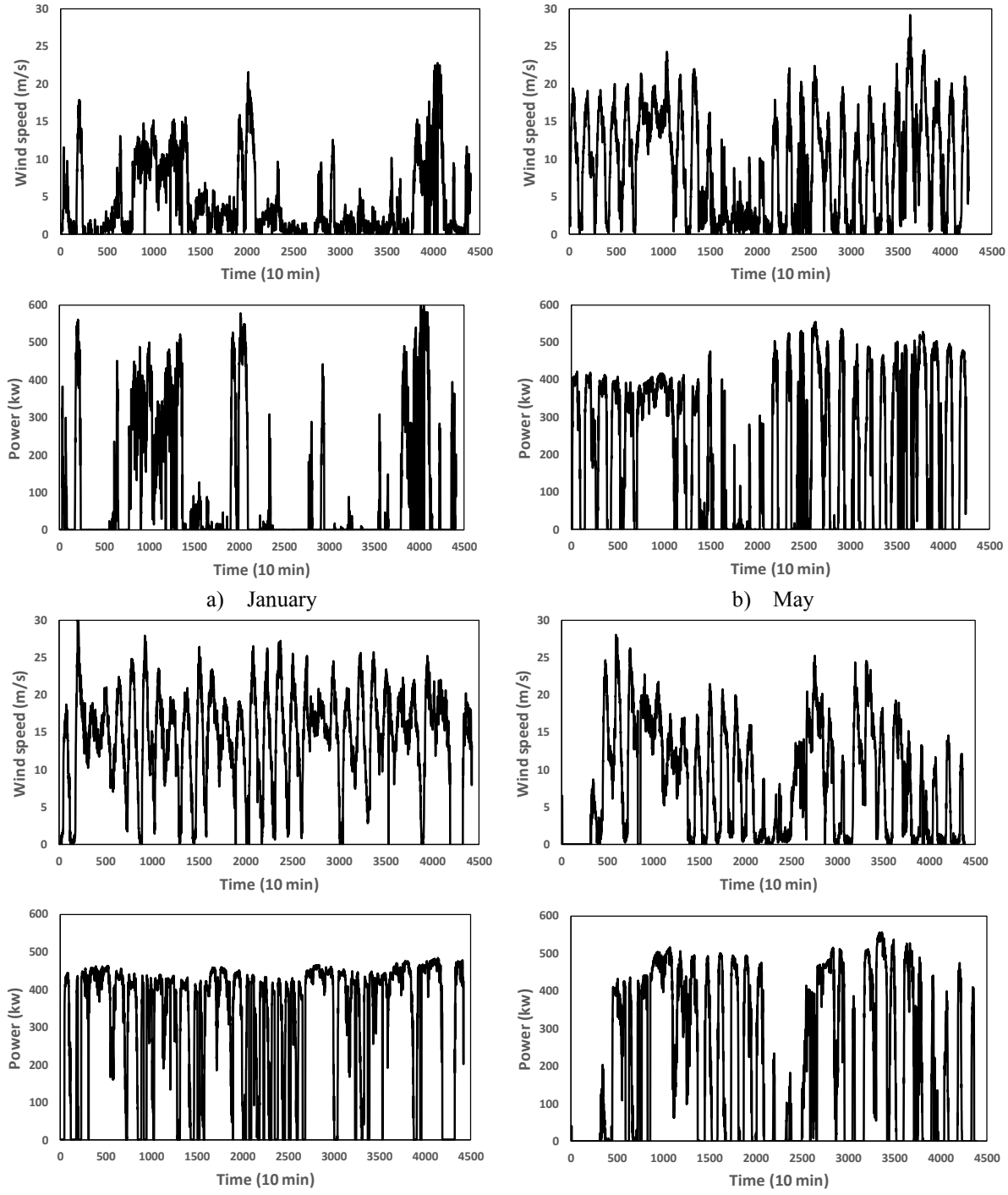

Fig. 9. Wind speed measured and power produced in T5 in sample months of January, May, July and October of 2013 according to SCADA data.

7. Conclusion

Due to the complex terrains of the mountainous region, the site of the Manjil wind farm has been a proper candidate to study according to the SCADA data and the numerical simulation results. In this regard, a numerical simulation was conducted using the actuator disk model in OpenFOAM. The simulation results for turbines wakes are similar to previous studies with ADM theory. The wake recovered in 10D of first-row turbines. Then, raw SCADA data was analyzed for wind assessment and compared to the simulation results.

The monthly analysis of SCADA wind data for the Manjil wind farm proved that most windy days with high energy potential occur in June, July, August, and September And there are only a few considerable windy days in winter. Harvested wind energy in January, May and October is around 31%, 63% and 66% of July, respectively. Thus suggested to switch off the wind farm in November, December, January and February to reduce loads, maintenance and operation cost. This strategy should be considered in levelized energy cost and other economic studies before wind farm construction (Majidniya et al, [18]).

Due to the specific location of the wind farm, the dominant wind blows from the north only. Therefore, it can be suggested to install turbines without yaw systems to reduce the investment cost.

From the simulation of the first-row turbine wakes, in 10D, there was still a wind deficit at the hub height of about 15% and 16% of incoming wind speed for case study 1 and case study 2, respectively, in a neutral atmospheric condition. For near wake,1D after the turbine, there are 58% and 56% speed reductions for case study 1 and case study 2 respectively. For the extension of the wind farm, the distance from the first row turbines should be either much larger than 10D or the second-row turbines should be installed between the wakes of the first row turbines. This seems possible due to the one-directional wind.

Acknowledgment

Sabz Manjil Electrical Power Plant Company is acknowledged for sharing their SCADA data.

References

[1] IPCC, (2014): Climate Change 2014: Synthesis Report. Contribution of Working Groups I, II and III to the Fifth Assessment Report of the Intergovernmental Panel on Climate Change [Core Writing Team, R.K. Pachauri and L.A. Meyer (eds.)]. IPCC, Geneva, Switzerland, 151 pp.

[2] Mattuella J, Loredo-Souza A, Oliveira M, Petry A. Wind tunnel experimental analysis of a complex terrain micrositing. Renewable and Sustainable Energy Reviews. 2016;54:110-9.

[3] Kuo JY, Romero DA, Beck JC, Amon CH. Wind farm layout optimization on complex terrains–Integrating a CFD wake model with mixed-integer programming. Applied Energy. 2016;178:404-14.

[4] Makridis A, Chick J. Validation of a CFD model of wind turbine wakes with terrain effects. Journal of wind engineering and industrial aerodynamics. 2013;123:12-29.

[5] Kozmar H, Allori D, Bartoli G, Borri C. Complex terrain effects on wake characteristics of a parked wind turbine. Engineering Structures. 2016;110:363-74.

[6] Castellani F, Vignaroli A. An application of the actuator disc model for wind turbine wakes calculations. Applied Energy. 2013;101:432-40.

[7] Choi NJ, Nam SH, Jeong JH, Kim KC. Numerical study on the horizontal axis turbines arrangement in a wind farm: Effect of separation distance on the turbine aerodynamic power output. Journal of Wind Engineering and Industrial Aerodynamics. 2013;117:11-7.

[8] Porté-Agel F, Wu Y-T, Lu H, Conzemius RJ. Large-eddy simulation of atmospheric boundary layer flow through wind turbines and wind farms. Journal of Wind Engineering and Industrial Aerodynamics. 2011;99(4):154-68.

[9] Yang X, Pakula M, Sotiropoulos F. Large-eddy simulation of a utility-scale wind farm in complex terrain. Applied energy. 2018;229:767-77.

[10] Castellani F, Astolfi D, Burlando M, Terzi L. Numerical modelling for wind farm operational assessment in complex terrain. Journal of Wind Engineering and Industrial Aerodynamics.2015;147:320-9.

[11] Frank HP, Rathmann O, Mortensen NG, Landberg L. The numerical wind atlas-the KAMM/WAsP method. 2001.

[12] Astolfi D, Castellani F, Garinei A, Terzi L. Data mining techniques for performance analysis of onshore wind farms. Applied Energy. 2015;148:220-33.

[13] Seim F, Gravdahl AR, Adaramola MS. Validation of kinematic wind turbine wake models in complex terrain using actual windfarm production data. Energy. 2017;123:742-53.

[14] Burton T, Sharpe D, Jenkins N, Bossanyi E. Handbook of wind energy. (No Title). 2001.
[15] Schmidt, J., Chang, C.Y., (2016). IWES tools for CFD site assessment M2T1: terrainBlockMesher. Fraunhofer IWES, Oldenburg, Germany.
[16] Schmidt, J., Chang, C.Y., (2016). IWES tools for CFD site assessment M2T2: addRotors +calcRotorDisks. Fraunhofer IWES, Oldenburg, Germany.
[17] Rai RK, Gopalan H, Sitaraman J, Mirocha JD, Miller WO. A code-independent generalized actuator line model for wind farm aerodynamics over simple and complex terrain. Environmental modelling & software. 2017;94:172-85.
[18] Majidniya M, Gharali K, Raahemifar K. A comparison of off-grid-pumped hydro storage and grid-tied options for an IRSOFC-HAWT power generator. International Journal of Rotating Machinery. 2017;2017(1):4384187.